Seasonal Dynamics of Green Hydrogen Supply and Demand: A Spatio Temporal Study of Freight Transport in Portsmouth City UK

Oghenovo Okpako†, Imran Usman Sumda†, Kelvin Anoh‡ and Haile-Selassie Rajamani†
†Department of Energy and Electronic Engineering, University of Portsmouth, United Kingdom
‡Centre for Future Technologies, University of Chichester, United Kingdom
†University of Wollongong, Dubai, United Arab Emirates
oghenovo.okpako@port.ac.uk, imran.sumda@port.ac.uk, k.anoh@chi.ac.uk, HaileRajamani@uowdubai.ac.ae

***Abstract*—The global effort towards decarbonising the transportation sector has intensified interests in hydrogen-based solutions, particularly in energy-intensive applications such as heavy goods vehicles (HGVs), where battery technologies may be limited. This study investigates the seasonal dynamics of green hydrogen supply powered by an offshore wind farm (OWF) and the demand of Portsmouth City freights, focusing on the year 2050. Using Geographic Information System (GIS) tools, locations for OWF and green hydrogen production facilities are identified by analysing offshore wind resource areas, proximity to transport routes, demand centres, and potential storage hub. Geospatial analysis was done using ArcGIS and Global Wind Atlas tools, while seasonal hydrogen production and demand are simulated using MATLAB. The results reveal a notable seasonal mismatch between hydrogen demand for logistics and road freight, and the supply of hydrogen generated by electrolysers. The seasonal mismatch in green hydrogen production and demand are used to propose a dynamic pricing model that incentivises hydrogen consumption during surplus periods while mitigating supply deficits. This work is important as it provides the foundation to investigate demand side management under freight transport.**

Keywords—Green hydrogen, Wind Energy, Heavy Goods Vehicles, Hydrogen Refueling Station, Dynamic Pricing.

I. INTRODUCTION

The United Kingdom (UK) is committed to Net-Zero carbon by the year 2050 as a consignee of the 2015 Paris convention agreement on combating global climate change. More urgently, the UK plans to liberate the UK families from the extortive energy costs of petrostates by using UK natural resources to generate all their electricity by 2030, a project referred to as Clean Power 2030 (CP2030). This coincides with the United Nations Sustainable Development target for 2030. In the CP2030 target, the UK expects hydrogen to contribute up to 10 GW to its energy mix. To achieve this goal, decarbonisation of key sector like the transport sector has been identified by the UK government [1]. Road freight transport, in particular, stands out as a critical sector in the decarbonisation effort due to its disproportionately large greenhouse gas (GHG) emissions relative to its fleet size. Whilst the use of battery technologies has been proposed as one of the key strategies to decarbonise the transport sector, their low energy density and the intense energy required by heavy goods vehicles (HGVs) for freight limits their use. In the UK, HGVs account for less than 2% of total vehicle population[2], but account for more than 20% of energy consumed and 16% emissions within the transport sector [3]. With diesel powering about 98.6% of the UK's HGV fleet, and the fleet size expected to increase by nearly 50% in 2050 [4], the need for clean fuel alternatives is obvious. The UK CCC 6th carbon budget identifies hydrogen as a key energy in decarbonising HGVs [1], [5]. Whilst blue and green hydrogen have been proposed to be the dominant shades of hydrogen in a future hydrogen economy, it is envisaged that green would play a key role in UK transport decarbonisation. This assertion is supported by the abundance of renewable energy resources like offshore wind, etc.

Green hydrogen, created through electrolysis of desalinated water by using electricity from renewable energy sources, is an alternative fuel for transport with zero GHG emission. In vehicles, water is the waste product of hydrogen as fuel. It is further supported by its shorter refuelling time and high energy density, making it suitable for long-distance and high-load applications [6].

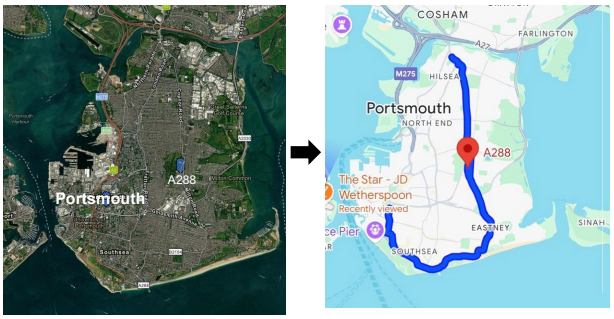

Fig. 1. A288 road in Portsmouth, United Kingdom.

Besides the environmental benefits of green hydrogen, it is cost effective when produced from curtailed renewable energy resources, and grid connection scenarios [7]. It is critical to understand the seasonal dynamics of hydrogen supply and demand, as it affects pricing, to assist consumers, suppliers, regulators and policymakers, etc. in the UK. Using Portsmouth City as a case study, this paper uses ArcGIS software-a

geospatial analytical tool to identify key offshore resource areas suitable for development of offshore wind farm (OWF) and hydrogen production whilst considering demand centers by using factors such as freight activities and roads for the Portsmouth City. Using Google map and ArcGIS, Fig. 1, shows the A288 road, a critical freight corridor in Portsmouth, having a concentration of HGV movement along the road. These transport pathways are critical for understanding regional hydrogen infrastructure requirements and the logistical viability of green hydrogen deployment.

Portsmouth City is located on the Southcoast of England, at approximately 50.8°N and 1.1°W. Its coastal location has proximity to the English Channel. Its exposure to the prevailing south-westerly winds makes it ideal for wind-powered renewable energy applications. These geographical qualities boost the possibility of electrolysis-based hydrogen production, especially when utilising offshore wind resources. Thus, an OWF Onshore hydrogen production system proposed by Catapult UK was considered in the model developed for this work [8]. In such a system, the electricity produced from a sole dedicated OFW is fed onshore to an electrolyser plant around the refueling station to produce hydrogen for meeting HGVs fleet demand in Portsmouth City around route A288.

II. System Model

This study proposes green hydrogen production based on wind energy from OWF areas of the UK, using Portsmouth city as an example. The model shown in Fig. 2, depicts a green hydrogen production system in which renewable energy from wind turbines is used to power the desalination plant, electrolyser and compressor.

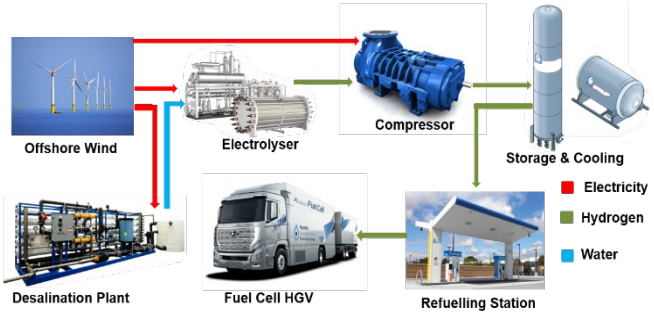

Fig. 2. Green Hydrogen Production, Storage and Consumption Systems.

In this study, hydrogen fuel is produced from the electrolysis of water from the widely available water bodies in Portsmouth. Water is first desalinised by removing any salt, before passing through the electrolyser to produce the hydrogen fuel that is stored and sold at the refueling stations used in driving HGVs.

A. HGV Fleet Analysis in Portsmouth

In this study, manual traffic count data for HGVs along the A288 route in Portsmouth, retrieved from the UK Department for Transport (DfT) [9], was utilised to establish a baseline for estimating the projected hydrogen demand in the year 2050. Aligned with the average distance travelled, the data provides a comprehensive framework for projecting future hydrogen demand. According to the DfT, an average of 98 HGVs travelled the A288 route daily in 2023 [9]. The seasonal average daily Vehicle Kilometer (VKM) travelled for HGVs was derived using quarterly national HGVs distance data for Great Britain in 2023 [10], serving as the secondary dataset for Portsmouth case study. The quarterly distances are aligned with the seasonal structure to capture temporal variations in operational patterns, reflecting changes in road conditions, weather, and logistical demand. To ensure accurate representation, a weighted average approach is employed, assigning proportional influence to each month based on its number of days within the season. This method effectively captures the relative contribution of longer and shorter months, resulting in a more representative distance metric for hydrogen demand analysis. Let $\{S\}_{i=1}^{s}$ denote a set of all the seasons and $\{M\}_{j=1}^{n}$ represent all the months in a year in the UK. The average daily VKM travelled by the HGVs in season i can be expressed as:

$$\Psi_i = \frac{\sum_{j=1}^{n} d(M_j)\psi(M_j)}{\sum_{j=1}^{n} d(M_j)}, \qquad i = 1, \dots, s \tag{1}$$

where $d(M_j)$ is the number of days in month j and $\psi(M_j)$ is the average daily VKM travelled by the HGVs in month j.

Let $\mathcal{N}_i$ be the total number of days in each season i so that,

$$\mathcal{N}_i = \sum_{\substack{M_j \in S_i \\ j \neq i}}^{n} d(M_j) \tag{2}$$

where $M_j \in S_i$ denote the months in season S_i. In the UK, there are four seasons (Winter, Spring, Summer and Autumn), each of these seasons is made up of three months. It follows that

$$S = \{\text{Winter, Spring, Summer, Autumn}\} \tag{3}$$

where $\text{Winter} = \{\text{Dec, Jan, Feb}\}$, $\text{Spring} = \{\text{Mar, Apr, May}\}$, $\text{Summer} = \{\text{Jun, Jul, Aug}\}$ and $\text{Autumn} = \{\text{Sept, Oct, Nov}\}$.

The number of days in month M_j was used as follows:

$$d(M_j) = \begin{cases} 31, & \text{if } M_j \in \{\text{Jan, Mar, May, Jul, Aug, Oct, Dec}\} \\ 30, & \text{if } M_j \in \{\text{Apr, Jun, Sep, Nov}\} \\ 28, & \text{if } M_j = \text{Feb.} \end{cases} \tag{4}$$

Thus, the total number of days in season S_i, e.g., Winter $\mathcal{N}_1 = 90$, Spring $\mathcal{N}_2 = 92$, Summer $\mathcal{N}_3 = 92$, and Autumn $\mathcal{N}_4 = 91$.

B. HGV Demand Estimation

To estimate the 2050 daily HGVs traffic volume on Route A288, a compound annual growth model is employed. The baseline traffic volume of 98 HGVs per day, based on current observational data for year 2023 in [9] is used. The future traffic projection is estimated using the following:

$$\mathcal{H}_{k+1} = \mathcal{H}_k(1 + r)^{\Delta t}, k = 0, 1, 2, \cdots \Delta t - 1 \tag{6}$$

where $\mathcal{H}_{k+1}$ is the projected future HGVs traffic, $\mathcal{H}_k$ is the present HGV traffic, r = annual growth rate assumed as 1.60%, Δt = number of years (i.e. year 2050 − 2023 = 27 years). Thus, the projected daily traffic volume on Route A288 by the year 2050 is 150. Using this projection, the hydrogen demand of the HGVs in kg in season S_i denoted as $\mathcal{D}_i$ is calculated as:

$$\mathcal{D}_i = \eta . \mathcal{H}_{k+1} . \mathcal{N}_i . \Psi_i \tag{7}$$

where η is the H_2 fuel economy of HGVs, that is 0.085kg/km.

C. Geospatial Analysis of Offshore Around Portsmouth

In the UK, Everoze Partners Ltd was commissioned by the Crown Estate to produce a comprehensive mapping of geographically suitable zones for the future deployment of OWFs within the territorial waters surrounding UK [11]. That project was implemented based on land availability, exclusion zones (e.g., airports, urban areas) and proximity to existing energy infrastructure. Consequently, this study uses ArcGIS software to identify offshore wind resource zones around Portsmouth city suitable for OWF as shown in Fig. 3, based on Everoze recommendation. The selected site was constrained to fixed-bottom foundation technologies, due to its comparative cost effectiveness over floating foundation alternatives. The proposed OWF site can be located in any of the identified area that spans ≈479.83 km². This area is centered at a latitude of 50.57° and longitude of -0.99°. Its centre point is 33.72 km from the A288 road corridor, offering strategic accessibility. This approach follows established best practices in spatial and energy system integration, as highlighted by [6]. The OWF size required was then scaled as follows:

$$A = \frac{\mathcal{W}.(W^{\mathrm{cw}}.L).(W^{\mathrm{dw}}.L)}{10^6} \tag{8}$$

where A is the area of the OWF site in km^2, $\mathcal{W}$ is the number of wind turbine considered, L is the rotor diameter of the wind turbine (in m), $W^{\mathrm{cw}} = 5$ and $W^{\mathrm{dw}} = 10$ are the dimensionless crosswind and downwind spacing respectively. They help prevent wake loss and ensure efficient utilisation of OWF space.

D. Wind Data

The Global Wind Atlas (GWA) version 3.4 was used to analyse the wind resources around the identified OWF site. The tool provides an accurate dataset for wind energy assessments and gives a decade-long record of average wind speeds at a specific site, as well as monthly wind speed index [12]. Thus, allowing for investigation of temporal wind variability. In order to evaluate the efficacy of the GWA wind data, validation was done. GWA validation against long-term historical meteorological records was carried out using data from a UK Met Mast located at the round 3 offshore wind energy development zone at Navitus bay. Root Mean Square Error (RMSE) and Mean Absolute Percentage Error (MAPE) were used to assess the validation. GWA wind data was provided at a hub height of 50 meters and it will be used as the reference height (h_1) for the wind resource assessment OWF location of this study. The average monthly wind speed was obtained by adjusting the average annual wind speed to the monthly wind speed index. Bonus B82/2300 offshore wind turbines are selected for this location. These turbines are typically installed at hub heights of 80–100 meters. Thus, the average monthly wind speed from GWA data was extrapolated to a hub height of 100 meters for the proposed OWF. Using the power law model, the expected wind speed, v_2, at the desired height ($h_2 = 100$ m) for each month of the year will be:

$$v_2 = v_1(h_2.h_1^{-1})^{\beta} \tag{9}$$

where v_1 is wind speed at h_1, $\beta = 0.11$ is wind shear exponent, which is often used for offshore areas [13].

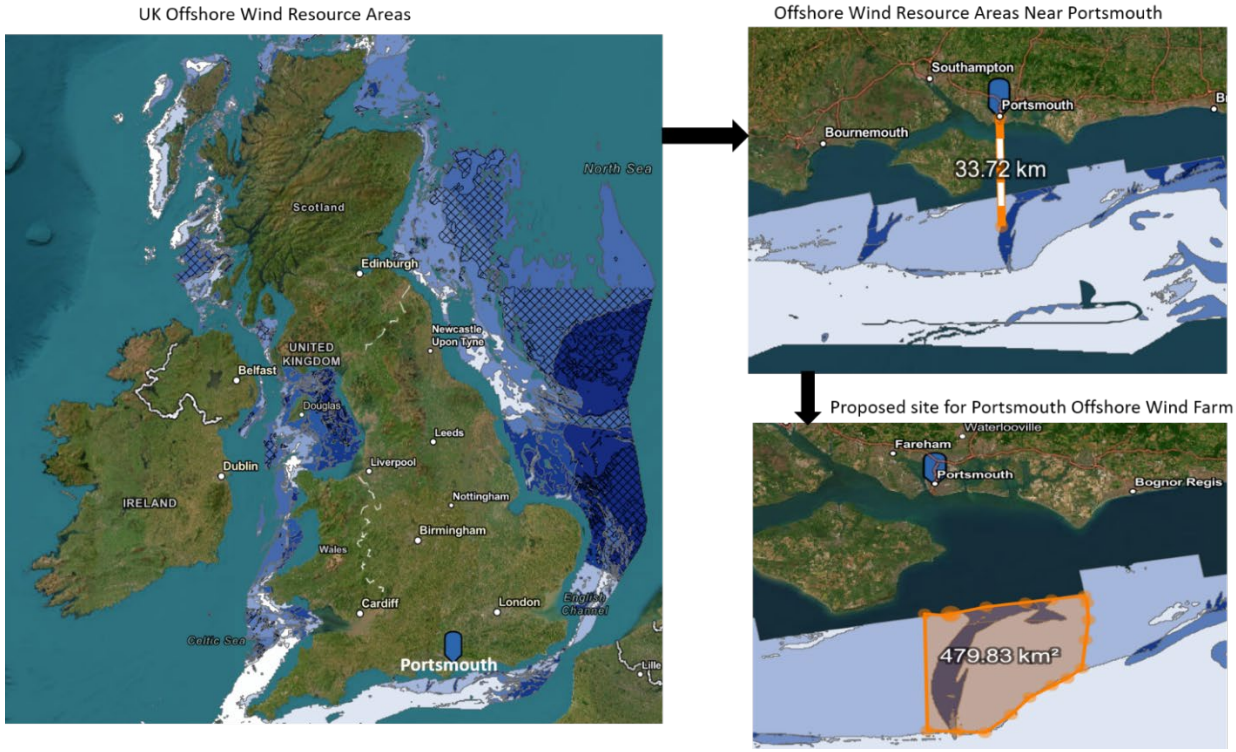

Fig. 3. Proposed Offshore wind farm site using ArcGIS software for Green Hydrogen Production.

E. Wind Turbine Power Curve

The Bonus B82/2300 2.3MW wind turbine selected for the proposed OWF, has its power curve serving as the basis for converting any given wind speed v to electrical power output $P(v)$. The power curve data was interpolated to a refined wind speed resolution (0–25 m/s) to facilitate accurate power output estimation. The resulting power curve is represented as a piecewise function, as outlined below:

$$P(v) = \begin{cases} 0, & v < v^{\text{Cut-in}} \\ P^{\text{Rated}}, & v^{\text{Rated}} \le v \le v^{\text{Cut-out}} \\ P^{\text{Rated}}.(\alpha)^3, & v^{\text{Cut-in}} \le v < v^{\text{Rated}} \\ 0, & v > v^{\text{Cut-out}} \end{cases} \quad (10)$$

where α is a dimensionless normalised wind speed that is between $v^{\text{Cut-in}}$ and v^{Rated}. In practice, α is calculated as:

$$\alpha = \frac{v - v^{\text{Cut-in}}}{v^{\text{Rated}} - v^{\text{Cut-in}}} \quad (11)$$

where $v^{\text{Cut-in}}$, $v^{\text{Cut-out}}$, and v^{Rated}, are the Cut-in, Cut-out and the rated speed of the wind turbine, respectively and P^{Rated} is the rated power output of the wind turbine.

F. Weibull Distribution and Expected Power Output

To accurately estimate wind turbine power output from monthly average wind speeds data used from GWA, the Weibull probability density function (PDF) was employed to account for wind speed variability at the OWF [14]. The Weibull PDF of the average monthly wind speed, $f(v)$, is found as:

$$f(v) = \frac{k}{c}\left(\frac{v}{c}\right)^{k-1} e^{-\left(\frac{v}{c}\right)^k} \quad (12)$$

where, k is shape factor, c is scale parameter. Using the annual average wind speed, v^{avg}, the scale parameter is realised from

$$c = \frac{v^{\text{avg}}}{0.9}. \quad (13)$$

The expected power output from the wind turbine, P^{Exp}, was calculated using the trapezoidal numerical integration method. That is, by integrating the wind turbine power curve weighed by the Weibull PDF, $f(v)$, then:

$$P^{\text{Exp}} = \int_{v=0}^{v^{\text{Cut-out}}} P(v) f(v) dv \quad (14)$$

where P^{Exp} also represents the available wind power. Not necessarily all this power will be consumed by the electrolyser. This study assumed the turbine was not shutdown in all seasons.

G. Electrolyser and Seasonal Hydrogen Supply

Electricity produced from the OWF was considered as the power source of the electrolysers. Three Nel-MC250, commercially available proton exchange membrane (PEM) electrolysers, were considered in this study to provide the hydrogen supply. Each electrolyser has a nominal power rating $P^{\text{Elect}}_{\text{rating}}$ of 1.25MW and an energy consumption per unit kg of H_2 produced (E_{H_2}) as 59 kWh/kg of H_2. The electrolysers hydrogen supply is dependent on P^{Exp}. They were powered by 3 Bonus B82/2300 wind turbine already discussed. It is likely to have scenario where the electricity produced from the OWF is greater than the electrolyser nominal power, particularly at high wind intensity. In such scenario, curtailment of the wind turbine is done to ensure that wind farm produces within the electrolyser capacity. Thus, the electrolyser power consumption in month j denoted as $P^{\text{Elect}}_{\text{Cons}}(M_j)$ is calculated as follows:

$$P^{\text{Elect}}_{\text{Cons}}(M_j) = \begin{cases} P^{\text{Exp}}(M_j), & \text{if } P^{\text{Exp}}(M_j) \le P^{\text{Elect}}_{\text{rating}} \\ P^{\text{Elect}}_{\text{rating}}, & \text{if } P^{\text{Exp}}(M_j) > P^{\text{Elect}}_{\text{rating}} \end{cases} \quad (15)$$

If $P^{\text{Exp}} > P^{\text{Elect}}_{\text{rating}}$, the OWF turbine is curtailed. The curtailed wind energy in season S_i denoted as $\mathcal{C}_i$ is calculated as:

$$\mathcal{C}_i = \sum_{\tau=0}^{\mathcal{T}-1}\sum_{j=1}^{n}\left(\xi(M_j).\ P^{Exp}(M_j) - P^{\text{Elect}}_{\text{rating}}\right).d(M_j,\tau) \quad (16)$$

$$\xi(M_j) = \begin{cases} 1, & P^{\text{Exp}}(M_j) > P^{\text{Elect}}_{\text{rating}} \\ 0, & P^{Exp}(M_j) \le P^{\text{Elect}}_{\text{rating}} \end{cases} \quad (17)$$

where $\xi(M_j)$ is the curtailment state of the OWF turbine in month M_j, assigned a logic of 0 or 1. The logic 1 signifies curtailment and 0 signifies non-curtailment. The hydrogen supply in kg in season S_i denoted as $\mathcal{S}_i$ can be obtained as:

$$\mathcal{S}_i = \frac{\sum_{\tau=0}^{\mathcal{T}-1}\sum_{j=1}^{n} d(M_j,t).P^{\text{Elect}}_{\text{Cons}}(M_j,t)}{E_{H_2}} \quad (18)$$

Here, $\mathcal{T} = 24$, is the hourly period of a day although it can be resolved according to the alternative periods of interest.

H. Seasonal Hydrogen Balance

For any season, S_i, the demand and supply of hydrogen fuel to drive HGVs must be satisfied to maintain an equilibrium in the market. Let $\mathcal{D}_i(\tau)$ represent the amount of H_2 required in season S_i and $\mathcal{S}_i(\tau)$ represent the amount of H_2 supplied during season S_i, both of which at time $\tau = 0,1,\cdots,\mathcal{T}-1$. To ensure a seasonal balance in the market, then

$$\sum_{\tau=0}^{\mathcal{T}-1}\sum_{M_j=1}^{n}\mathcal{D}_i(M_j,\tau) = \sum_{\tau=0}^{\mathcal{T}-1}\sum_{M_j=1}^{n}\mathcal{S}_i(M_j,\tau), i = 1,\cdots,s. \quad (19)$$

On the other hand, let $\mathcal{E}_i(\tau)$ denote the amount of excess hydrogen fuel in season S_i. It forms a crucial rationale for the dynamic seasonal pricing proposed in this study. The excess H_2 supply can be expressed as:

$$\mathcal{E}_i(\tau) = \mathcal{D}_i(\tau) - \mathcal{S}_i(\tau), \qquad \tau = 0,1,\cdots,\mathcal{T}-1. \quad (20a)$$

To control the demand for H_2 in the market, a penalty is assigned, for example,

$$\begin{cases} \mathcal{E}_i(\tau) > 0, & \text{discount is applied} \\ \mathcal{E}_i(\tau) < 0 & \text{penalty is applied} \\ \mathcal{E}_i(\tau) = 0, & \text{price is unchaged} \end{cases} \quad (20b)$$

Its output can be classified into excess, deficit, or balanced supply. The absolute value of $\mathcal{E}_i(\tau)$, that is $|\mathcal{E}_i(\tau)|$, and $\mathcal{D}_i(\tau)$ are both used to quantify the magnitude of the green hydrogen supply and demand mismatch in % in season S_i For example, let

$$\mathcal{B}_i(\tau) = \frac{|\mathcal{E}_i(\tau)|}{\mathcal{D}_i(\tau)} \times 100 \quad (21)$$

where $\mathcal{B}_i(\tau)$ depicts the mismatch between $\mathcal{E}_i(\tau)$ and $\mathcal{D}_i(\tau)$.

I. Hydrogen Market and Proposed Dynamic Pricing

Traditionally, the hydrogen markets at the wholesale level has been driven through long term contracts, future contracts, power purchase agreements, and fixed pricing. But, fixed pricing does not reflect the variation in renewable generation, the market demands, weather, social factors, across seasons. Thus, to cater for these factors, the concept of dynamic pricing for green hydrogen market is proposed in this work. Dynamic pricing allows the adjustment of hydrogen price based on real-time market conditions. Using the base hydrogen price ϖ, the proposed H_2 fuel price in S_i denoted as $\omega_i(\tau)$ is calculated as:

$$\omega_i(\tau) = \begin{cases} \varpi.\theta_1^i(\tau), & \text{if } \mathcal{E}_i(\tau) > 0 \\ \varpi.\theta_2^i(\tau), & \text{if } \mathcal{E}_i(\tau) < 0 \\ \varpi, & \text{if } \mathcal{E}_i(\tau) = 0 \end{cases} \quad (22)$$

where $\theta_1^i(\tau)$ and $\theta_2^i(\tau)$ are adjustment factors applied to the ϖ under surplus and deficit conditions, respectively, for notational simplicity. These factors depend on the penalty (ϕ), discount (χ), utilisation sensitivity (γ), and seasonal variation sensitivity (λ) factors. Each of these parameters are defined as:

$$\theta_1^i(\tau) = (1 - \chi.\mathcal{B}_i(\tau)).(1 - \gamma.u_i(\tau)).(1 - \lambda \cdot \varphi_i) \quad (23)$$

$$\theta_2^i(\tau) = (1 + \phi.\mathcal{B}_i(\tau))(1 + \gamma(1 - u_i(\tau))).(1 + \lambda.\varphi_i) \quad (24)$$

where $u_i(\tau)$ is the electrolyser utilisation factor in season S_i, and φ_i quantifies the extent to which the supply deviates from the mean as a proportion of the mean value. A high φ_i suggests greater seasonal fluctuation, potentially indicating high volatility in supply and the need for storage and demand response strategies to mitigate supply inconsistencies. Both $u_i(t)$ and φ_i are expressed as follows:

$$u_i(\tau) = \frac{\sum_{j=1}^{n} P_{\text{Cons}}^{\text{Elect}}(m_j)}{n.P_{\text{Rating}}^{\text{Elect}}} \quad (25)$$

$$\varphi_i(\tau) = \frac{\sigma_i(\tau)}{\mu_i(\tau)}, \tau = 0,1,\cdots,\mathcal{T}-1 \quad (26)$$

σ_i is the standard deviation of hydrogen supply across all seasons (in kg). μ is the mean hydrogen supply across all seasons (in kg). where the cardinality $|S|$. In order to carry out this investigation, the dynamic pricing parameters were set to empirically grounded values reflective of UK offshore wind-driven hydrogen production by 2050: ϖ = £6/kg, χ = 0.25, ϕ = 0.30, γ= 0.25, and λ = 0.25. These values fall within literature-supported ranges for base price, penalty and discount adjustments during seasonal imbalance[15], utilisation sensitivity based on electrolysers performance [16], and seasonal production variability from offshore wind [17].

III. Results and Discussion

Fig. 4. Show's the wind speed validation based on 2001 to 2011 data. It can be seen that the wind speed is highest during the winter months/seasons. It has a correlation coefficient of 0.95, RMSE value of 0.52 m/s, and MAPE value of -0.01 m/s.

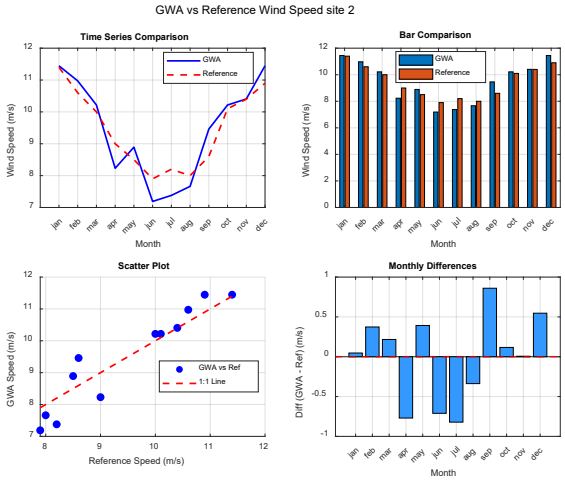

Fig.4. Wind speed validation of the proposed dynamic pricing data.

The results in Fig. 4. justify the reliability of the GWA wind data used in this study. Fig.5, is the Bonus B82/2300 wind power curve. Using the Weibull wind speed, the cut in and cut out speed for are 3.5 m/s and 25 m/s respectively. Fig. 6, shows the seasonal hydrogen supply in terms of surplus or deficit. It can be seen that there is a seasonal mismatch between the hydrogen supply and demand. There is a surplus hydrogen during winter and autumn, and there is a deficit hydrogen supply during summer and spring. This is mainly due to the wind fluctuation.

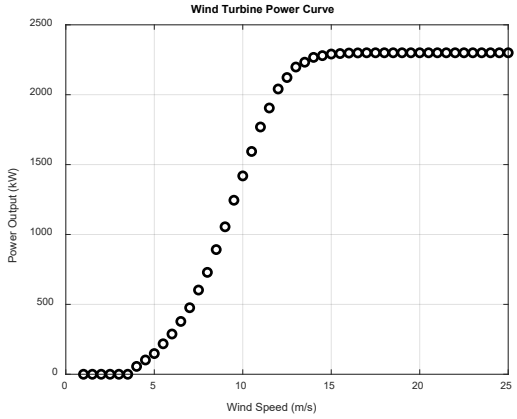

Fig.5. Wind turbine power curve.

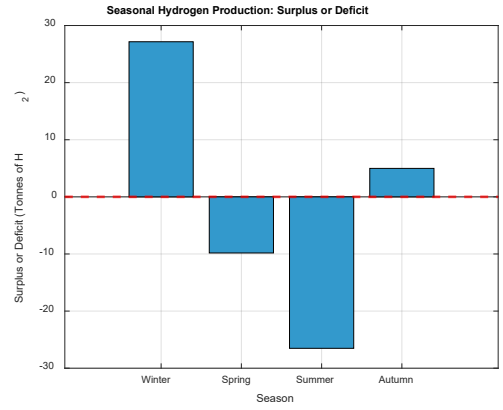

Fig. 6. Results of seasonal hydrogen production/supply surplus or deficit by 2050 in Portsmouth.

This result clarifies the seasonal variation between hydrogen supply and demand. Whilst increasing the electrolyser capacity would reduce deficit spring and summer, on the other hand it would increase oversupply during winter and autumn. Also increasing the capacity of the wind turbine would result to curtailment and energy wastage. This variation and problems emphasise the need for storage and demand response program for green hydrogen. In such a system, the excess hydrogen is stored during the Winter and Autumn and used for meeting the deficit during Summer and Spring. Dynamic pricing has a key role to play in this, as it would encourage consumers within the transportation sector, among others to shift flexible consumption to when there is surplus hydrogen supply. Fig. 6, is the sensitivity analysis of the dynamic pricing model. It can be seen that ϕ and γ are the most sensitive scaling factor. Fig. 7, is the seasonal hydrogen price. As seen from the graph the prices of hydrogen is low during the winter and autumn and is high during the summer and spring compared to the base price. The low-price of hydrogen during winter months is attributed to the high wind speed leading to a high utilisation of the electrolysers.

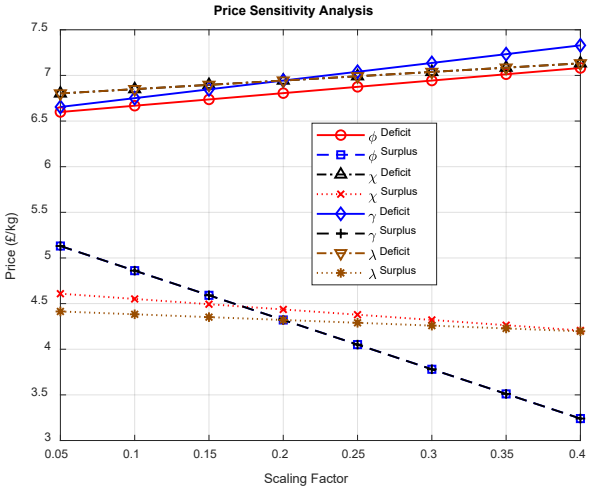

Fig.7. Sensitivity of scaling factors for dynamic seasonal pricing of green hydrogen in Portsmouth OWF study area.

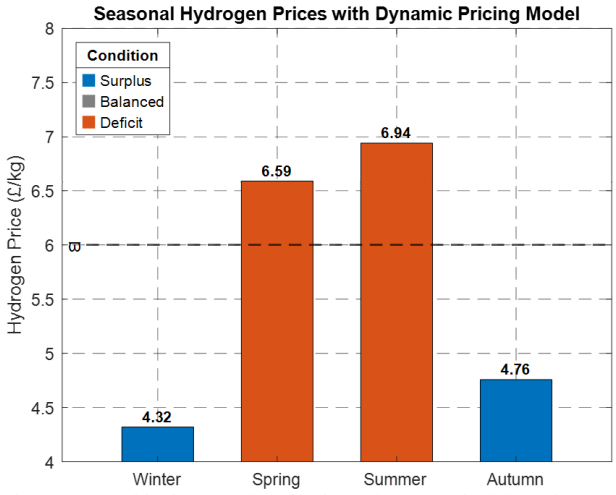

Fig. 8. Seasonal hydrogen prices for dynamic seasonal pricing of green hydrogen in Portsmouth OWF study area.

IV. Conclusion

In this study, the potential for green hydrogen usage for HGVs in Portsmouth UK for the year 2050 has been investigated using UK DfT data, GIS tools and MATLAB. The results show a seasonal mismatch between the hydrogen supply and demand. The developed dynamic pricing model provides the platform to further investigates how Demand Side Management could become attractive for hydrogen consumers in transport, as it reflects real-time market conditions where the prices of hydrogen reflects the seasonal variation between hydrogen supply and demand, and consumers could schedule their hydrogen usage based on price. The findings further provide developers of green hydrogen refuelling station, policymakers, and business investors both practical and theoretical insights of how pricing and hydrogen storage is critical for driving the UK's 2050 net-zero carbon freight and Clean Power 2030 transformations. Whilst hydrogen consumer's behavioural change based on price could have associated discomfort, this study provides the platform on which such can be further investigated. To support the effectiveness of dynamic pricing for green hydrogen in Portsmouth for year 2050, government role, local community engagement, and consumer's education is very key. Plug Power company is championing this pricing concept.

References

[1] Climate Change Committee, "*Policies for the Sixth Carbon Budget and Net Zero,*" 2020. Available: www.theccc.org.uk/publications. Accessed: May 22, 2025

[2] UK Department for Transport, "*Vehicle Licensing Statistics Data Tables*," GOV.UK, 2025. [Online]. Available: https://www.gov.uk/government/statistical-data-sets/vehicle-licensing-statistics-data-tables. Accessed: May 22, 2025

[3] UK Department for Transport, "*Greenhouse Gas Emissions from Transport in 2023*," 2025. [Online]. Available: https://www.gov.uk/government/statistics/transport-and-.Accessed: May 22, 2025

[4] UK Department for Transport, "*Greenhouse Gas Emissions from Transport in 2022,"* 2024. [Online]. Available: https://www.gov.uk/government/statistics/transport-and-environment-statistics-2024/greenhouse- .Accessed: May 22, 2025.

[5] HM Government, *The Ten Point Plan for a Green Industrial Revolution, London*, UK: HM Government, 2020.

[6] M. Minutillo, A. Perna, A. Forcina, S. Di Micco, and E. Jannelli, "Analyzing the levelized cost of hydrogen in refueling stations with on-site hydrogen production via water electrolysis in the Italian scenario*," Int. J. Hydrogen Energy*, vol. 46, no. 26, pp. 13667–13677, Apr. 2021,doi: 10.1016/j.ijhydene.2020.11.110.

[7] J. Park et al., "Green hydrogen to tackle the power curtailment: Meteorological data-based capacity factor and techno-economic analysis," *Appl. Energy,* vol. 340, Jun. 2023, doi: 10.1016/j.apenergy.2023.121016.

[8] D. Wallace, G. Smart, K. Stefaniak, S. Mann, Z. Kurban, et al., "OSW-H2: *Solving the Integration Challenge*," 2020.

[9] UK Department for Transport, "*Road Traffic Statistics*: *Manual Count Point 36908*," 2025. [Online]. Available: https://roadtraffic.dft.gov.uk/manualcountpoints/3690 Accessed: May 22, 2025.

[10] UK Department for Transport, "*Domestic Road Freight Activity (RFS01),*" GOV.UK, 2025. [Online]. Available: https://www.gov.uk/government/statistical-data-sets/rfs01-goods-lifted-and-distance-hauled . Accessed: May22, 2025.

[11] Everoze, *Broad Horizons: Key Resource Areas for Offshore Wind Summary Report*, The Crown Estate, 2020.

[12] N. N. Davis et al., "The Global Wind Atlas: A high-resolution dataset of climatologies and associated web-based application*," Bull. Amer. Meteorol. Soc*., vol. 104, no. 8, pp. E1507–E1525, 2023 doi: 10.1175/BAMS-D-21-0075.1.

[13] G. Jeans, "Converging profile relationships for offshore wind speed and turbulence intensity," *Wind Energy Sci*., vol. 9, no. 10, pp. 2001–2015, Oct. 2024. doi: 10.5194/wes-9-2001-2024.

[14] G. C. Efthimiou, D. Hertwig, S. Andronopoulos, J. G. Bartzis, and O. Coceal, "A statistical model for the prediction of wind-speed probabilities in the atmospheric surface layer," *Boundary-Layer Meteorol.,* vol. 163, no. 2, pp. 179–201, May 2017. doi: 10.1007/s10546-016-0221-2.

[15] HM Government, *UK Hydrogen Strategy, London, UK: Dandy Booksellers Ltd, 2021.*

[16] U.S. Department of Energy, "*U.S. Department of Energy Hydrogen Program: 2023 Annual Merit Review and Peer Evaluation Report*," Jun. 2023.

[17] Carbon Brief, *"Energy*," 2025. [Online]. Available: https://www.carbonbrief.org/energy/ Accessed: May 22, 2025.